On Phase Transitions in the Early Universe

Hans-Otto Carmesin[1,2,3] and Philipp Schöneberg[1]

[1]Gymnasium Athenaeum, Harsefelder Straße 40, 21680 Stade
[2]Studienseminar Stade, Bahnhofstr. 5, 21682 Stade
[3]Universität Bremen, Fachbereich 1, Postfach 330440, 28334 Bremen
hans-otto.carmesin@t-online.de

Kurzfassung

Die kontinuierliche Ausdehnung des Raums seit dem Big Bang ist eine großartige Entdeckung der Menschheit. Allerdings ist diese kontinuierliche Ausdehnung unvollständig, denn sie kann nicht die physikalischen Vorgänge bei sehr hoher Dichte und hoher Energie der Quanten der Strahlung beschreiben. In diesem Aufsatz lösen wir dieses Problem der Unvollständigkeit, indem wir ein Tröpfchenmodell entwickeln und analysieren: Tröpfchen einer Dimension bilden sich und wachsen, sowie die Dichte eine entsprechende kritische Dichte unterschreitet. Bei diesem dimensionalen Phasenübergang nehmen Abstände sehr schnell zu. Als Konsequenz wird das Horizontproblem gelöst.

Abstract

The continuous expansion of space since the Big Bang has been a great discovery of mankind. However, that continuous expansion is incomplete, as it fails to describe the physics at very high density and high energy of radiation quanta. In this paper, we provide a solution of that incompleteness problem by developing and analyzing a droplet model: Droplets of a dimension form and grow, as soon as the density falls below a corresponding critical density. At that dimensional phase transition, the light horizon increases in an extremely rapid manner. As a consequence, the horizon problem is solved.

1. Introduction

Students are highly interested in astronomy and astrophysics (Elster 2010, Jenkins 2006, Pössel 2015). This includes the time evolution of space since the Big Bang. Basically, that time evolution is described as an expansion of space according to general relativity, GR. However, Guth (1981) pointed out that this description is problematic, as there occurs a horizon problem as well as a flatness problem. Thus, the description of the increase of space since the Big Bang is incomplete, see Fig. (1). The horizon problem can be overcome by a very rapid enlargement of distances in the very early universe. For it, Guth (1981) proposed an era of 'cosmic inflation'. However, the proposed mechanism of 'cosmic inflation' is also problematic, as there occurs a reheating problem (Broy, 2016) and a fine-tuning problem, see e. g. Landsman (2016), Carmesin (2019a, p. 187). In fact, the era of rapid enlargement occurs in a natural manner as a consequence of dimensional phase transitions. Thereby, these transitions occur naturally at high density in the early universe (see e. g. Carmesin, 2017, 2019a, 2021a). Accordingly, the student's interest in the era of 'cosmic inflation' and in dimensional phase transitions is founded. So, such transitions provide a basis for a substantial didactical perspective.

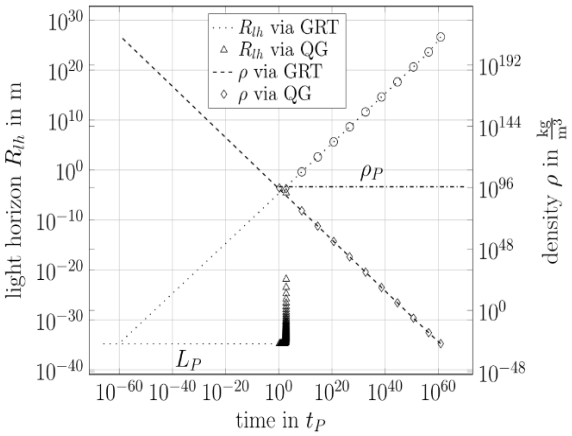

Fig. 1: Time evolution of the light horizon R_{lh} and of the density ρ as a function of time in Planck times t_P according to general relativity, GRT, and corresponding to quantum gravity, QG, (see Carmesin 2020a, Fig. (5.7) or Carmesin 2021b, Fig. (2.4)): At the Big Bang, the light horizon starts at approximately the Planck length, $R_{lh} \approx L_P$. Then the light horizon increases slightly by the formation of vacuum, and it increases extremely rapidly at a series of dimensional phase transitions, without the formation of vacuum (triangles, this process is described by quantum gravity). Later, the light horizon increases in three-dimensional space purely by the formation of vacuum (circles, only this process is described by general relativity, GR or GRT. Altogether, GRT is incomplete, as it describes the expansion of space only in the later universe.

1.1. Didactical perspective

The didactical perspective can be analysed in the framework of the didactical triangle, see Franke and Gruschka (1996) or Fig. (2). That triangle represents the relation between the students, the teacher and the subject. Hereby, the relation between the students and the subject is characterized by a high interest of the students, including the motivating aspect of scientific curiosity, see Fig. (3).

According to the didactical triangle, the role of the teacher becomes essential. The teacher should take care of the following expectations: Firstly, the students expect answers. Secondly, some advanced students expect methods, so that they can achieve answers on their own. The present project was developed in a research club. Thereby, the teacher provides a course in quantum gravity for especially interested students. Moreover, research projects are provided, coached and overseen by the teacher. In this manner, separate scientific questions and corresponding skills for the treatment of these questions are provided, see Fig. (4).

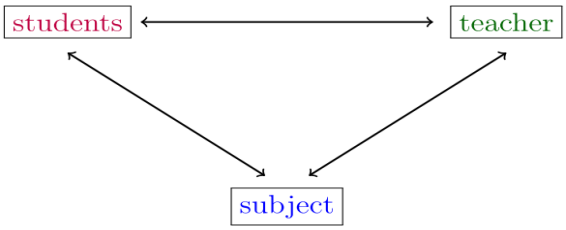

Fig. 2: Didactical triangle.

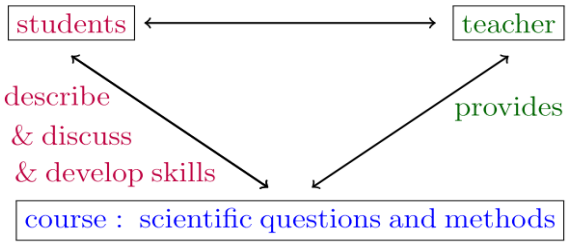

Fig. 3: Didactical triangle: course enables students to perform research project

Furthermore, in the case of the present project, the student Philipp Schöneberg and the teacher Hans-Otto Carmesin agreed to collaborate. Such collaborations have been performed several times in the recent years, see Carmesin (2021f). Thereby, tasks for the teacher and for the student are clearly separated. In the present case, the teacher developed the analytic investigation of the droplet model, while the student provided a numerical study of the model, a study of the solution of the horizon problem by the droplet model and the development of graphical representations of droplets at various dimensions.

1.2. Didactical perspective of vacuum

In order to understand the formation of droplets at a dimensional phase transition, the teacher presented that concept and dynamics of formation of vacuum to learners ranging from class 8 to 13 in the research club (Carmesin, 2021f). Then, the students were able to describe and discuss the steps of the respective derivations and to discuss the consequences, Fig. (3).

In particular, the students realized the following items: Firstly, the dynamics of vacuum have been tested. Secondly, dimensional phase transitions are a natural consequence of the dynamics of vacuum. Thirdly, higher dimensional physics has been observed in experiments (Lohse et al. 2018, Zilberberg et al. 2018). Fourthly, dimensional phase transitions naturally provide the era of cosmic inflation. Fifthly, the critical densities have been derived and evaluated. Sixthly, these critical densities explain the everyday life fact of three-dimensional space (D = 3 is non-trivial and requires an explanation). On the other hand, the students pointed out that the concept of a dimensional phase transition is surprising. Moreover, the students developed skills, so that they were able to solve a research project, see Fig. (4).

Altogether, this course combined with the projects provides several didactical perspectives, see Fig. (4).

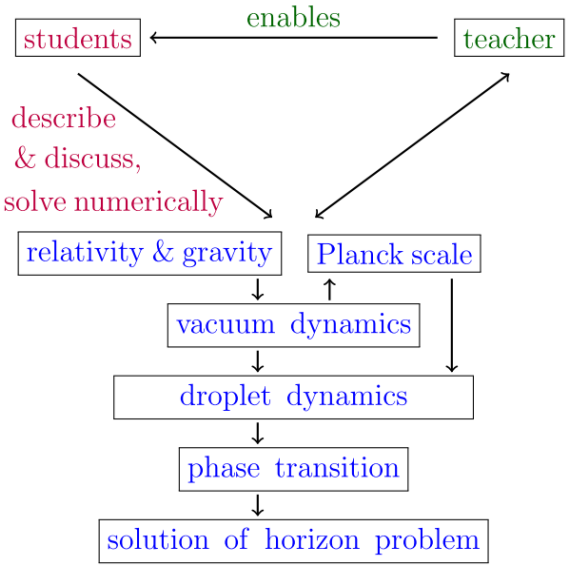

Fig. 4: Didactical triangle illustrates students describing, discussing and providing numerical solutions in the research club.

1.3. Description of the scientific problem

The expansion of the universe since the Big Bang has been observed by various methods (see e. g. Wirtz 1924, Hubble 1929, Penzias and Wilson 1965, Efstathiou et al. 2020, Pesce et al. 2020, Riess et al. 2016, 2021, Philcox et al. 2020, Addison et al. 2018, Abbot et al. 2020, Birrer et al. 2020, Escamillae-Rivera and Najera 2021, Blakeslee 2021, Suzuki et al. 2011). Moreover, that expansion has been modelled on the basis of general relativity (see e. g. Einstein 1905, 1915, 1917, Friedman 1922, Lemaitre 1927, Carmesin 2019a-b, 2020a-b, 2021a-f). However, these models are not complete, see Fig. (1):

A comprehensive physical theory is characterized by the combination of gravity and quantum physics (Carmesin 2022a-c). In that framework of quantum gravity, physical systems range from small size at the Planck length $L_P = 1.616 \cdot 10^{-35}$m to the present-day light horizon at $R_{lh} = 4.1 \cdot 10^{26}$ m. Moreover, the Planck density $\rho_P = 5.155 \cdot 10^{96}$ kg/m^3 cannot be exceeded in nature (Carmesin 2021a). Naturally, in a comprehensive physical system, the Planck length can be achieved. However, according to general relativity combined with the Planck scale, the time evolution of the present-day light horizon does not include radii smaller than 0.001 mm, as at that radius, the corresponding density of the universe would be equal to the Planck density, so a further reduction of R_{lh} would be impossible, see Fig. (1), Carmesin (2020a). According to an advanced analysis within quantum gravity, the above incompleteness of GRT is solved, thereby the light horizon has reached the Planck length, $R_{lh}(t) \approx L_P$. This is achieved by a series of dimensional phase transitions (see e. g. Carmesin 2017, 2018a-c).

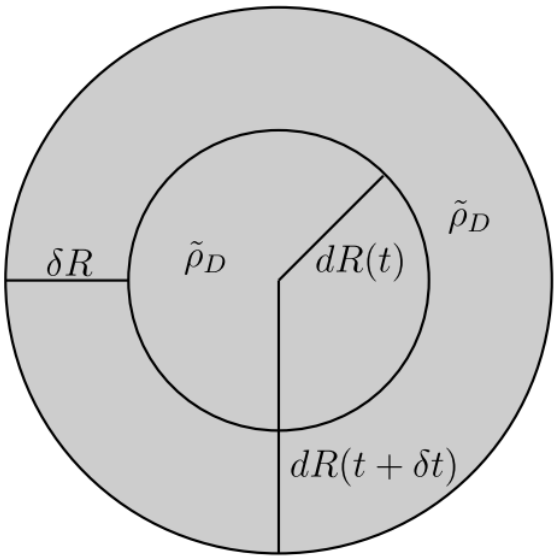

Fig. 5: Droplet model: A droplet with radius dR(t) forms additional vacuum according to quantum gravity and corresponding to the expansion of space in the universe. Simultaneously, the droplet loses vacuum, as the vacuum propagates at the velocity of light. We consider the droplet in possibly higher dimensional space or surroundings, so there is no flow of vacuum into the droplet that could compensate for the outflow. If the formation of vacuum in the droplet exceeds the outflow of vacuum from the droplet, then the droplet is stable and the corresponding dimension can form via the growth of such droplets.

So far, these phase transitions have been derived by four methods: a van der Waals type analysis of two objects (see e. g. Carmesin 2017, 2018a-c, van der Waals 1873), a transition in a Bose gas (see e. g. Carmesin 2021a, Bose 1924, Sawitzki and Carmesin 2021), a phase transition of connections (see e. g. Carmesin 2021a) and a theory of the dark energy (see e. g. Carmesin 2018a-c, 2021a-b).

In this paper, we apply the droplet model to provide a fifth derivation of the phase transitions in the early universe. The droplet model is a very powerful physical tool, as it provides a very clear and convincing analysis and since it is very intuitive, in addition. Accordingly, droplet models have been used in various fields of science very successfully: in nuclear physics (Gamov 1930, v. Weizsäcker 1935), in fluid dynamics (Sirignano 2009), in biology (Zwicker et al. 2016), in thermodynamics, and hydrodynamics (Sidin 2009), for instance.

2. **Droplet Model**

In this section, we apply the droplet model to dimensional phase transitions in the early universe. Thereby, we often use Planck units, and we mark these by a tilde (Carmesin 2019a, 2021a).

In our droplet model, a droplet represents a ball in D dimensional space, see Fig. (2). We analyse the change δR of the radius dR(t) of the droplet during a time interval δt, see Fig. (2). Accordingly, there occurs a change δV of the volume dV of the droplet. The d in dR should mark that dR can be very small. Similarly, dV can be very small.

Thereby, the volume dV is the volume of the ball at a time t and with a radius dR. Hereby, we denote the volume of a ball with radius one in D dimensions by V_D. So, the volume of the ball is as follows:

$$dV(t) = V_D \cdot dR(t)^D \qquad \{1\}$$

During a time interval δt, the radius of the ball increases by δR. Thus, the new volume of the ball is as follows:

$$dV(t+\delta t) = V_D \cdot (dR+\delta R)^D \qquad \{2\}$$

Hence, the volume of the formed vacuum is the volume of the shell in Fig. (2):

$$\delta V = \delta V_{shell} = dV(t+\delta t) - dV(t)$$
$$= V_D \cdot [(dR+\delta R)^D - dR^D] \qquad \{3\}$$

Thence, the formed vacuum gives rise to the following relative increase of the volume of the droplet in Fig. (2):

$$\delta V/dV = V_D \cdot [(dR+\delta R)^D - dR^D]/[V^D \cdot dR^D]$$
$$= (1+\delta R/dR)^D - 1 = \varepsilon \qquad \{4\}$$

Hereby and in general, we denote a relative change of volume by ε as follows:

$$\delta V/dV = \varepsilon \qquad \{5\}$$

Accordingly, the rate of change of the volume in a time interval δt is the ratio of ε and δt:

$$\text{Rate}(\varepsilon) = \varepsilon/\delta t \qquad \{6\}$$

So, the formed vacuum gives rise to the following rate:

$$\text{Rate}(\varepsilon) = [(1+\delta R/dR)^D - 1]/\delta t \qquad \{7\}$$

It is well known, according to GRT, that the expansion of space since the Big Bang is caused by the density $\tilde{\rho}_{D=3}$ in three-dimensional space. Similarly, the rate at which vacuum forms is caused by the density $\tilde{\rho}_D$ in D dimensional space. The rate of that formation of vacuum has been derived in the framework of quantum gravity as follows, see equation (3.46) in (Carmesin 2021a):

$$\text{Rate}(\varepsilon_{\text{formation}}) = D^{1/2} \cdot (2\cdot\tilde{\rho}_D)^{(D-1)/4}/\delta t \qquad \{8\}$$

The vacuum formed in the droplet propagates at the velocity of light c, as otherwise, it would be possible to measure a velocity v < c of an object relative to the vacuum. However, it is impossible to measure such a velocity v < c relative to the vacuum or relative to space, according to relativity (Einstein 1905, Carmesin 2019a, 2021a, 2018a-c). So, the vacuum propagates outwards out of the droplet, see Fig. (2), at the velocity c. Thus, the vacuum propagating outwards fills a shell with the following thickness:

$$\delta R = c\cdot\delta t \qquad \{9\}$$

So, the droplet with radius dR becomes a droplet with radius dR – δR. Hence the volume moving outwards is as follows:

$$\delta V = \delta V_{\text{shell}} = V_D\cdot[dR^D - (dR - \delta R)^D]$$

Thence, the vacuum propagating outwards has the following relative volume:

$$\delta V/dV = V_D\cdot[dR^D - (dR - \delta R)^D]/[V^D\cdot dR^D]$$

$$= 1 - (1 - \delta R/dR)^D = \varepsilon_{\text{out}} \qquad \{10\}$$

Thus, the corresponding rate is as follows:

$$\text{Rate}(\varepsilon_{\text{out}}) = [1 - (1 - \delta R/dR)^D]/\delta t \qquad \{11\}$$

At the critical density $\tilde{\rho}_{D,c}$, the droplet just begins to grow. At this begin of growth of the droplet, the rate of outflowing vacuum Rate(ε_{out}) is equal to the rate of formation of vacuum Rate($\varepsilon_{\text{formation}}$):

$$\text{Rate}(\varepsilon_{\text{out}}) = [1 - (1 - \delta R/dR)^D]/\delta t$$

$$= D^{1/2} \cdot (2\cdot\tilde{\rho}_{D,c})^{(D-1)/4}/\delta t = \text{Rate}(\varepsilon_{\text{formation}}) \qquad \{12\}$$

That equation is solved for $(2\cdot\tilde{\rho}_{D,c})$ as follows:

$$2\cdot\tilde{\rho}_{D,c} = [1 - (1 - \delta R/dR)^D]^{4/(D-1)} \cdot D^{-2/(D-1)} \qquad \{13\}$$

For simplicity, we apply the abbreviations q = δR/dR and $x = 2\cdot\tilde{\rho}_{D,c}$. So the equation for the critical density is as follows:

$$x = [1 - (1 - q)^D]^{4/(D-1)} \cdot D^{-2/(D-1)}$$

$$\text{with } x = 2\cdot\tilde{\rho}_{D,c} \quad \text{and } q = \delta R/dR \qquad \{14\}$$

Next, we analyse the time evolution of the density, see Fig. (1).

3. Calculations of the critical densities

In this section, we use Eq. {14} to calculate the critical densities for different droplet radii dR in which they become unstable. For it, we start by using the biggest droplet with the radius $dR = R_{lh}$ of the light horizon radius so we can analyse the critical densities of the universe. Because we want to compare the results of this droplet with the whole spectrum of droplets, we also calculate the critical densities of the smallest droplet with the radius dR of one Planck length. Moreover, we examine some further examples with a relative thickness q of the shell (see Eqs. {15,16}) of 0.5, 0.25, 10^{-1}, 10^{-2}, 10^{-3}, 10^{-4}, and 10^{-5} to have a greater spectrum of droplets to compare with. So, we obtain the radius:

$$dR = \frac{\delta R}{q} \qquad \{15\}$$

In particular, we may imagine the case $\delta R = L_P$. So, the radius is as follows:

$$d\tilde{R} = \frac{dR}{L_P} = \frac{1}{q} \qquad \{16\}$$

constants:

q	1

D	**x**
3	3.33E-01
4	3.97E-01
5	4.47E-01

Fig. 6: Part of the spreadsheet used to calculate critical densities at dimension D. For instance, for the case q = 1.

Here and in the following, we mark a quantity by a tilde, if that quantity is represented in Planck units. For calculating the different critical densities to every chosen droplet, for each dimension, we use a Microsoft Excel spreadsheet (Fig. 6), where we include Eq. {14} and use the chosen droplets as a function of the variable q. Furthermore, we represent the scaled critical densities x as a function of the dimension D (Fig. 4).

Fig. (7) shows that relatively small droplet radii $d\tilde{R} = \frac{1}{q}$ have relatively high critical densities for every dimension. In particular, the time evolution of the droplet with the size of the light horizon corresponds to the smallest droplets in the early universe, while it corresponds to the largest droplets in the late universe.

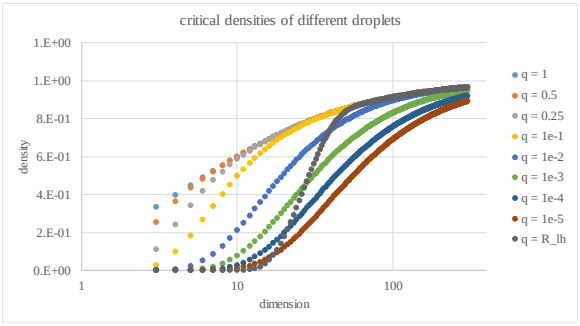

Fig. 7: Scaled critical densities x as a function of the dimension D for various relative thicknesses q.

4. Geometry of the vacuum droplets

The light horizon radius corresponds to different droplet sizes at different times, according to the dynamics based on the geometry and the characteristics of the vacuum. One of these dynamics is described by the vacuum outflow, flowing into every space direction. At a dimensional transition, the number of these directions changes, see Fig. (8).

So, the directions of the vacuum outflow and the emitting vacuum change too. These dynamics have an impact on the stability of the droplet. The second dynamics are based on the fact, that mass or dynamical mass creates vacuum. Since the vacuum has this characteristic too, the vacuum droplets grow through their own mass or dynamical mass. This increases the stability of a droplet. In combination these two dynamic effects are balanced at the critical density or droplet radius. Because vacuum droplets at high dimension have many space directions, they have a relatively small size combined with a relatively big surface. Thus, such small droplets are stable at high density only. At low dimension these dynamics can stabilize only big droplets. So, when the density decreases during the time evolution after the Big Bang, then there occur dimensional transitions at which a high dimensional droplet changes to a low dimensional droplet. Hereby, the low dimensional droplet can be interpreted as a sheet, compared to the high dimensional droplet, see Fig. (8). In this sense, the transition can be interpreted as a delamination of droplets. The inverse transition can be interpreted as a lamination of droplets. In this manner, dimensional transitions can occur.

5. Solution of the Horizon Problem

In this section, we solve the horizon problem. For it, we analyse the path propagated by light and the radius of the light horizon as a function of time. The radius is related to the density. Accordingly, we derive the scaled density x as a function of time. For this purpose, we apply a generalized version of the Friedmann-Lemaitre equation, see equation (2.424) in (Carmesin 2019a):

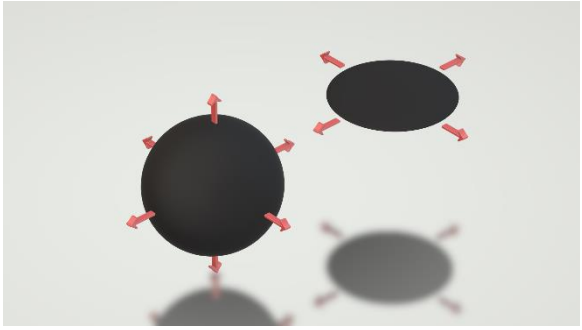

Fig. 8: The directions of the vacuum outflow, symbolized for the physically possible three-dimensional space and for the physically impossible two-dimensional space.

$$\frac{dx}{dt} = -(D+1)\cdot x^{\frac{D^2+5D+6}{4D+4}} \qquad \{17\}$$

We abbreviate the exponent by b:

$$\frac{dx}{dt} = -(D+1)\cdot x^{b} \qquad \{18\}$$

Now we separate the variables. For it, we multiply by dt and divide by x^b:

$$\frac{dx}{x^b} = -(D+1)\cdot dt \qquad \{19\}$$

Next, we form the indefinite integral:

$$\int \frac{dx}{x^b} = \int -(D+1)\cdot dt \qquad \{20\}$$

We evaluate both integrals:

$$\frac{1}{-b+1}\cdot x^{-b+1} = -(D+1)\cdot t \qquad \{21\}$$

Subsequently, we simplify:

$$x^{-b+1} = -(D+1)\cdot(b-1)\cdot t \qquad \{22\}$$

Next, we abbreviate the exponent by a, $a = -b+1$, and we abbreviate the term $-(D+1)\cdot(b-1)$ by d, $d = -(D+1)\cdot(b-1)$. So, we get the two invariants a and d at each dimension D. Thus, we derive the following equation:

$$x^a = d \times t \qquad \{23\}$$

We divide by t:

$$\frac{x^a}{t} = d \qquad \{24\}$$

We consider this equation for a time t_1 and a corresponding scaled density x_1 as well as for a time t_2 and a corresponding scaled density x_2. Using the invariant d, we derived the following equation:

$$\frac{x_{t_1}^a}{t_1} = d = \frac{x_{t_2}^a}{t_2} \qquad \{25\}$$

Subsequently, we can use the reciprocal fractions, and multiply by x_1^a:

$$\frac{t_1}{x_{t_1}^a} = \frac{t_2}{x_{t_2}^a} \qquad \{26\}$$

$$t_1 = \frac{t_2 \cdot x_{t_1}^a}{x_{t_2}^a} \quad \{27\}$$

Finally, we express the equation as follows:

$$t_1 = t_2 \cdot \left(\frac{x_{t_1}}{x_{t_2}}\right)^a \quad \{28\}$$

Next, we derive the path ds propagated by light during a time dt:

$$ds = c \cdot dt \quad \{29\}$$

We apply that Eq. to the time interval dt starting at the time of the last phase transition t_1 and ending at the time of the next dimensional phase transition t_2:

$$dt = t_2 - t_1 \quad \{30\}$$

Subsequently, we derive the expansion of the path ds as a consequence of the expansion of the universe. In the present case, the expansion takes place during the time interval starting at t_1 and ending at the present-day time t_0. Accordingly, we multiply the distance $ds(t_1) = ds_1$ by the ratio of the present-day radius of the light horizon, $R_{lh}(t_0) = R_{lh,0}$, and the radius of the light horizon at that time t_1 of the interval dt, $R_{lh}(t_1) = R_{lh,1}$. So, we use the following equation:

$$ds_{1,expanded} = ds_1 \cdot \frac{R_{lh,0}}{R_{lh,1}} \quad \{31\}$$

We integrate equation {31}:

$$\int ds_{1,expanded} = \int ds \cdot \frac{R_{lh,0}}{R_{lh,1}} \quad \{32\}$$

We evaluate both integrals. Because the interval dt between two phase transitions is relatively small, the ratio is approximately constant and we obtain the following equation:

$$s_{2,expanded} - s_{1,expanded} = c(t_2 - t_1)\frac{R_{lh,0}}{R_{lh,1}} \quad \{33\}$$

In order to calculate the distance $s_{total,2}$ at a time t_2, we add the additional distance $s_{2,expanded}$-$s_{1,expanded}$ to $s_{total,1}$:

$$s_{total,2} = s_{total,1} + s_{2,expanded} - s_{1,expanded} \quad \{34\}$$

In order to calculate the fraction in the above equation, we analyse the present-day light horizon and the values at earlier times, according to the expansion of the universe: For the case of a constant mass, the following relation holds:

$$R_{lh,1}^D \cdot x_1 = R_{lh,2}^D \cdot x_2 \quad \{35\}$$

However, in the early universe, the space was filled with radiation. Accordingly, the density x_1 is proportional to the radius $R_{lh,1}^{-(D+1)}$, corresponding to the redshift. So, the following equation holds:

$$R_{lh,1}^{D+1} \cdot x_1 = R_{lh,2}^{D+1} \cdot x_2 \quad \{36\}$$

Subsequently, we solve for $R_{lh,1}$:

$$R_{lh,1} = R_{lh,2} \cdot \left(\frac{x_2}{x_1}\right)^{\frac{1}{(D+1)}} \quad \{37\}$$

Fig. 9: Cubic model of the light horizon at the dimension D = 3. A ball has the radius L_P. The light horizon is the distance between the centres of balls of both ends. So, the light horizon corresponds to two L_P, see (Schöneberg and Carmesin 2020).

Since the calculations depend on an earlier value of the light horizon radius, it is necessary to know the first value. Observable objects are limited by the Planck scale. So, the light horizon radius cannot be smaller than two observable objects, see Fig. (9) (Schöneberg and Carmesin 2020).

So, for the first phase transition we apply the following equation:

$$\tilde{R}_{lh,300} = 2 \cdot \left(\frac{x_{300}}{x_{301}}\right)^{\frac{1}{(300+1)}} \quad \{38\}$$

However, because of the speed of light, the length of two Planck lengths can only be reached in two Planck times. So, accordingly the time of the first phase transition has to be $t_{301} = 2$ Planck times. For example, t_{300} is calculated as follows, see equation {28}:

$$\tilde{t}_{300} = 2 \cdot \left(\frac{x_{t_{300}}}{x_{t_{301}}}\right)^a \quad \{39\}$$

The possible radii of the droplets range from the Planck length to the light horizon. In the following, we perform two investigations: (1) The time evolution of the distance achieved by light for the case of the smallest droplet, and (2) the time evolution of the distance achieved by light for the case of the largest droplet. We develop a spreadsheet in order to perform investigation (1) and investigation (2), see Figs. (10 until 11).

D	x	$\tilde{t}$	$\tilde{R}\_lh$	s_expanded	s_total
3		2.51E+56	2.56E+58	7.53E+64	3.39E+69
3		4.41E+50	2.56E+55	1.32E+62	3.39E+69
3		4.41E+44	2.56E+52	1.32E+59	3.39E+69
			break in table		
299	9.62E-01	2.03E+00	2.00E+00	6.14E+64	7.81E+66
300	9.63E-01	2.02E+00	2.00E+00	6.08E+64	7.75E+66
301	9.63E-01	2.00E+00	2.00E+00	7.69E+66	7.69E+66

Fig. 10: Investigation (1) of the smallest droplet: Part of the spreadsheet to calculate the light horizon radius $\tilde{R}_{lh}$ and the distance covered by light s_{total} based on the scaled critical densities x, the time $\tilde{t}$ and dimension D for the smallest droplet radius.

In this table we calculate recursively beginning at the highest dimension D = 301 and leading to the lowest dimension D = 3. We present the dimensions in column 1, see Fig. (10). Secondly, for each dimension D, we calculate the scaled critical density x according to equation {14} and present the result in column 2, see Fig. (10). Thirdly, for dimension D = 301, we apply two Planck times according to equation {39}. The times are presented in column 3, and the unit is the Planck time. Fourthly, for dimension D = 300, we calculate the time according to equation {28} by using the time of dimension D = 301. Fifthly, and for each dimension D < 300, we calculate the time t recursively according to equation {28}. Sixthly, for dimension D = 301, we apply the light horizon at the Planck scale $R_{lh,301}$ = 2 Planck lengths according to equation {38}. These radii are presented in column 4, and the unit is the Planck length. Seventhly, for dimension D = 300, we calculate the length according to equation {37} by using the value of the light horizon radius of dimension D = 301. Eighthly, and for each dimension D < 300, we calculate the radius R_{lh} recursively according to equation {37}. Ninthly, we determine the distance achieved by light in two steps. First, we evaluate all distances between two phase transitions by using equation {33}, see column 5 in Fig. (10). Thereby, we use the values of column 4 according to equation {33}. Next, we determine the complete path covered by light by calculating the total of all of these paths, according to equation {34}. The results are presented in column 6, see Fig. (10).

Tenthly, for the expansion of the universe in three-dimensional space, we proceed as follows:

(10a) We take the time values corresponding to Fig. (2.23) in (Carmesin 2019a).

(10b) We take the values of the light horizon radius corresponding to Fig. (2.23) in (Carmesin 2019a).

(10c) We calculate s_{total} according to equation {34}. Investigation (1) of the smallest droplet as well as investigation (2) of the largest droplet, see Figs. (7-10) show that the total distance achieved by light is essentially larger than the light horizon radius. Moreover, we performed additional investigations with intermediate droplet sizes, whereby we obtained the same result:

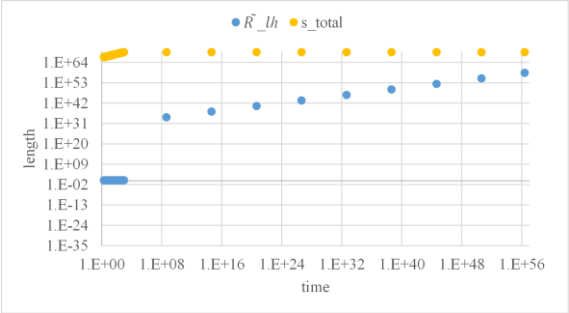

Fig. 11: Investigation (1) of the smallest droplet: Radius $\tilde{R}_{lh}$ and the distance covered by light s_{total} as a function of time $\tilde{t}$.

D	x	$\tilde{t}$	$\tilde{R}\_lh$	s_expanded	s_total
3	2.26E-60	4.91E+77	3.04E+12	1.24E+132	1.24E+132
4	3.98E-30	1.68E+51	8.34E+04	1.55E+113	1.55E+113
5	3.38E-18	1.27E+38	3.43E+02	2.85E+102	2.85E+102
			break in table		
299	9.62E-01	2.03E+00	2.00E+00	6.14E+64	7.81E+66
300	9.63E-01	2.02E+00	2.00E+00	6.08E+64	7.75E+66
301	9.63E-01	2.00E+00	2.00E+00	7.69E+66	7.69E+66

Fig. 12: Investigation (2) of the largest droplet: Part of the Spreadsheet to calculate the light horizon radius $\tilde{R}_{lh}$ and the distance covered by light s_{total} based on the scaled critical densities x, the time $\tilde{t}$ and dimension D for the droplet with the radius of the light horizon radius.

The total distance achieved by light is essentially larger than the light horizon radius. Altogether, our numerical studies show in a convincing manner that the horizon problem is solved in the framework of our droplet model.

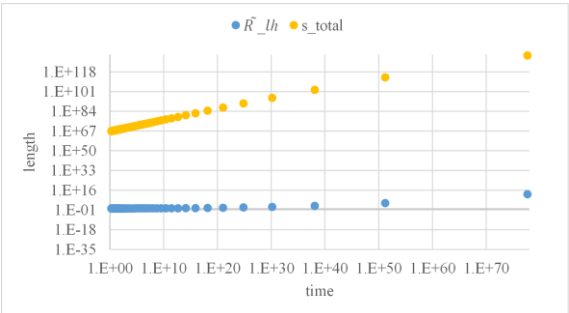

Fig. 13: Investigation (2) of the largest droplet: Radius $\tilde{R}_{lh}$ and the distance achieved by light s_{total} as a function of time $\tilde{t}$.

6. Experience with teaching

In our research club, we provide a combination as follows: A first partition provides the possibility to perform a research project in a coached and overseen manner. A second partition provides a course on quantum gravity, see Carmesin 2021f. In the second partition, the students are enabled to describe and discuss the presented derivations. Additionally,

the students can develop skills in that course. Some students of the second partition perform a research project. Hereby, they have the choice to perform the project on their own, or to perform a combined project with the teacher. In the latter case, the parts of student and teacher are clearly separated.

In the first partition of the research club, the students can choose topics different from quantum gravity, and most students do so.

Moreover, students can present their results in a public astronomy evening at the assembly hall.

Altogether, in that system, many students improved their skills significantly and achieved good results at the public presentations, at the discussions in the course and in the Jugend forscht competitions, see e. g. Carmesin (2021f).

7. Conclusion

In this paper, we address the incompleteness problem that the continuous expansion of space since the Big Bang, according to general relativity theory, does not describe the complete time evolution of the light horizon ranging from the Planck scale to the present-day light horizon, see Fig. (1).

That problem has been solved by a series of discontinuous phase transitions in the early universe (Carmesin 2019a, 2021a). While these phase transitions have been modeled by four methods so far, we present a fifth model: the droplet model. This model has essential advantages: it is intuitive, robust, can be solved exactly, and it has already been applied successfully in various fields of science.

We base our analysis on the basic dynamics of the vacuum (Carmesin 2019a, 2021a, 2022a). With it, we derive the critical densities for phase transitions as a function of the radius of the droplets in equation {14} and Fig. (7). Using these critical densities, we derive the time evolution of distances achieved in the universe by propagating light. We show that these distances are large compared to the light horizon, so that the light was able to thermalize the universe. In this manner we solve the horizon problem in addition to our solution of the incompleteness problem.

The experience with teaching shows that advanced students can use the combination of course and project, in order to achieve especially innovative results. Moreover, that system provides a high degree of individual learning: Students can choose a project according to their individual interests. Students can choose a presentation at the astronomy evening, without Jugend forscht competition or with competition. Students can choose the additional course and a corresponding project, so that synergies arise. Students can perform a project on their own, in a team with students or in a team with the teacher, only depending on their individual interests.

8. Literature

Abbott, T. M. C. et al. (2020). Dark Energy Survey Year 1 Results: Cosmological Constraints from Galaxy Clustering and Weak Lensing, Phys. Rev. D, 102, pp 1-34.

Addison, G. E. et al. (2018). Elucidating ΛCDM: Impact of Baryon Acoustic Oscillation Measurements on the Hubble Constant Discrepancy, ApJ, 853(2), pp 1-12.

Birrer, S. et al. (2020). TDCOSMO: IV. Hierarchical time-delay cosmography - joint inference of the Hubble constant and galaxy density profiles. Astronomy and Astrophysics, 643, pp. 1-40.

Blakeslee, J. P. et al. (2021). The Hubble Constant from Infrared Surface Brightness Fluctuation Distances, The Astrophysical Journal, 911(65), pp 1-12.

Bose, S. (1924). Plancks Gesetz und Lichtquantenhypothese, Z. f. Physik, 26, pp 178-181.

Broy, Benedict Johannes (2016). Inflation and effective Shift Symmetries. Hamburg, University Hamburg.

Carmesin, Hans-Otto (2017): Vom Big Bang bis heute mit Gravitation – Model for the Dynamics of Space. Berlin: Verlag Dr. Köster.

Carmesin, Hans-Otto (2018a). Universal Model for the Dynamics of Space, Dark Matter and Dark Energy. Berlin: Verlag Dr. Köster.

Carmesin, Hans-Otto (2018b). Theory for the Emergence of Space, Dark matter, Dark Energy and Space-Time. Berlin: Verlag Dr. Köster.

Carmesin, Hans-Otto (2018c): A Model for the Dynamics of Space - Expedition to the Early Universe. PhyDid B Internet Journal, pp. = 1-9.

Carmesin, Hans-Otto (2019a): Die Grundschwingungen des Universums - The Cosmic Unification. Berlin: Verlag Dr. Köster.

Carmesin, Hans-Otto (2019b): A Novel Equivalence Principle for Quantum Gravity. PhyDid B, pp. 17-25.

Carmesin, Hans-Otto (2020a): The Universe Developing from Zero-Point-Energy - Discovered by Making Photos, Experiments and Calculations. Berlin: Verlag Dr. Köster.

Carmesin, Hans-Otto (2020b): Explanation of the Rapid Enlargement of Distances in the Early Universe. PhyDid B, p. 1-9.

Carmesin, Hans-Otto (2021a). Quanta of Spacetime Explain Observations, Dark Energy, Graviton and Nonlocality. Berlin: Verlag Dr. Köster.

Carmesin, Hans-Otto (2021b). Cosmological and Elementary Particles Explained by Quantum Gravity. Berlin: Verlag Dr. Köster.

Carmesin, Hans-Otto (2021c). Physical Explanation of the H_0 – Tension. International Journal of Engineering and Science Invention (IJESI), 10(8) II, pp 34-38. Doi:10.35629/6734-1008023438

Carmesin, Hans-Otto (2021d). The Elementary Charge Explained by Quantum Gravity. Berlin: Verlag Dr. Köster.

Carmesin, Hans-Otto (2021e): The Origin of the Energy. PhyDid B, p. 29-34.

Carmesin, Hans-Otto (2021f): Lernende erkunden die Raumzeit. Der Mathematikunterricht 67(2), pp 47-56.

Carmesin, Hans-Otto (2022a). Quantum Physics Explained by Gravity and Relativity. Berlin: Verlag Dr. Köster.

Carmesin, Hans-Otto (2022b). The Electroweak Interaction Explained by and Derived from Gravity and Relativity. Berlin: Verlag Dr. Köster.

Carmesin, Hans-Otto (2022c). Geometric Derivation of the Spectrum of Vacuum. International Journal of Engineering and Science Invention (IJESI), 11(4) I, pp 1-11. Doi:10.35629/6734-1104010111

Efstathiou, G. et al. (Planck Collaboration) (2020). Planck 2018 results VI. Cosmological parameters, Astronomy and Astrophysics, 641(A6), pp 1-67.

Einstein, Albert (1905). Zur Elektrodynamik bewegter Körper. Annalen der Physik, 17, pp 891-921.

Einstein, A. (1915). Die Feldgleichungen der Gravitation, Sitzungsberichte der Königlich Preußischen Akademie der Wissenschaften, 1915, 844-847.

Einstein, A. (1917). Kosmologische Betrachtungen zur allgemeinen Relativitätstheorie, Sitzungsberichte der Königlich Preußischen Akademie der Wissenschaften, pp 142-152.

Elster, Doris (2010). Zum Interesse Jugendlicher an den Naturwissenschaften. Ergebnisse der ROSE Erhebung aus Deutschland und Österreich. Online-Publication: Shaker.

Escamilla-Rivera, C. and Najera, A. (2021). Dynamical dark energy models in the light of gravitational-wave transient catalogues, Journal of Cosmology and Astroparticle Physics 2022(3), pp 60-85.

Franke, Michael; Gruschka, Andreas (1996). Didaktische Bilder als Bilder der Didaktik. Pädagogische Korrespondenz 17, pp 52-62.

Gamov, G. (1930). Mass Defect Curve and Nuclear Constitution, Proceedings of The Royal Society A: Mathematical, Physical and Engineering Sciences, 126, pp 632-644.

Guth, Alan (1981). Inflationary universe: A possible solution to the horizon and flatness problems, Physical Review D 23, pp 347-356.

Hubble, E. (1929). A relation between distance and radial velocity among extra-galactic nebulae, Proc. of National Acad. of Sciences, 15, pp 168-173.

Jenkins, E.W. and Pell, R.G. (2006) The Relevance of Science Education Project (ROSE) in England: a summary of findings. Centre for Studies in Science and Mathematics Education, University of Leeds.

Landsman, Klass (2016). The Fine-Tuning Argument: Exploring the Improbability of Our Existence. Berlin: Springer.

Lohse, M. et al. (2018). Exploring 4D Quantum Hall Physics with a 2D Topological Charge Pump. Nature 553, pp 55-58.

Penzias, A. and Wilson, R. W. (1965). A measurement of excess antenna temperature at 4080 Mc/s, Astrophysical Journal Letters, 142, pp 419-421.

Pesce, D. W. et al. (2020). The megamaser cosmology project: XIII. Combined Hubble constant constraints, Astrophysical Journal Letters, 891, pp L1.

Philcox, O. Ivanov, M., Simonovic, M. and Zaldarriaga, M. (2020). Combining Full-Shape and BAO Analyses of Galaxy Power Spectra: A 1.6 % CMB-Independent Constraint on H0, arXiv, 2002.04035v3, pp 1-42.

Pössel, Markus (2015). Studien zum Interesse von Schüler/innen an Astronomie. Online-Publikation: Spektrum.

Riess, A. G. et al. (2021). Cosmic Distances Calibrated at 1 % Precision with Gaia EDR3 Parallaxes and Hubble Space Telescope Photometry of 75 Milky Way Cepheids Confirm Tension with ΛCDM, The Astrophysical Journal Letters, 908(L6), pp 1-11.

Riess, A. G. et al. (2016). A 2.4 % Determination of the Local Value of the Hubble Constant, The Astrophysical Journal, 826(1), pp 1-65.

Suzuki, N. et al. (2011). The Hubble Space Telescope Cluster Supernova Survey: V. Improving the Dark Energy Constraints above z > 1 and Building an Early-Type-Hosted Supernova Sample, ApJ, 746, pp 85-105.

Sawitzki, Paul and Carmesin, Hans-Otto (2021): Dimensional Transitions in a Bose Gas. PhyDid B, p. 53-59.

Schöneberg, Philipp and Carmesin, Hans-Otto (2020). Solution of a Density Problem in the Early Universe. PhyDid B, pp 43-46.

Schöneberg, Philipp and Carmesin, Hans-Otto (2021): Solution of the Horizon Problem. PhyDid B, p. 61-64.

Sirignano, W. A. (2009). Fluid Dynamics and Transport of Droplets and Sprays. Cambridge: Cambridge University Press.

Sidin, R. S. R. (2009). Droplet size distribution in condensing flow. Enschede: University of Twente.

van der Waals, J. D. (1873). Over de Continuiteit van den gas- en vloeistoftoestand, Leiden: Sijthoff.

v. Weizsäcker, C. F. (1935). Zur Theorie der Kernmassen, Zeitschrift f. Physik A, 96, pp 431-458.

Wirtz, C. (1924). Aus der Statistik der Spiralnebel, Astronomische Nachrichten, 222, pp 33-48.

Zilberberg, O. et al. (2018). Photonic topological pumping through the edges of a dynamical four-dimensional quantum Hall system. Nature 553, pp 59-63.

Zwicker, D. et al. (2016). Growth and division of active droplets provides a model for protocells, Nature Physics, 13, pp 408-414.

9. **Acknowledgements**

We thank Paul Sawitzki, Jonas Lieber, Kimberly Böttcher and Matthias Carmesin for interesting discussions and I. Carmesin for helpful discussions and proofreading the manuscript. We thank Daphne Carmesin for proofreading the manuscript.